express
polymer letters

Research article

Comparative assessment of cutting processes in the mechanical behavior of basalt fiber/poly(lactic acid) matrix composites

Varikkadinmel Binaz[ID]*, Kaushik Deepak*[ID]*, Inderdeep Singh*[*][ID]

Mechanical and Industrial Engineering Department, Indian Institute of Technology Roorkee, Uttarakhand, India

Abstract. To be used in semi-structural applications, the components of sustainable composites must have good mechanical properties and excellent dimensional/geometrical integrity, both of which are influenced by secondary processing techniques. Less emphasis has been placed on the development, mechanical/microstructural characterization, and secondary processing of sustainable basalt fiber/poly(lactic acid) composites (BFPLA), which can be an excellent choice for semi-structural applications. The present investigation aims to determine the best cutting process to create samples from BFPLA, as well as to experimentally evaluate the effect of different cutting processes (scroll sawing, computer numerical control (CNC) milling, water jet cutting, and abrasive water jet cutting (AWJ)) on the tensile and flexural properties of samples. Stereomicroscopy and field-emission scanning electron microscope (FE-SEM) are used to assess and correlate the influence of surface defects caused by cutting methods with mechanical behavior. AWJ machining consistently generated uniform surface profiles across all specimens, with minimum thermal degradation and fiber roll-out. Compared to the tensile strength values of unidirectional longitudinal, transversal, and bidirectional samples cut using milling, AWJ specimens exhibited a percentage increase of 27.9, 70.2, and 54.4%, respectively. It has been concluded that the choice of cutting technique has a significant impact on the strength of cut samples.

Keywords: biodegradable polymers, mechanical properties, material testing, machining processes, basalt fiber

1. Introduction

The ever-growing global plastic usage and contamination issues, added with the increased consumption of single-use plastics during the pandemic, have necessitated the development of sustainable and green solutions and their expanded applications [1]. That is where the employment of sustainable/compostable plastics and their composites, especially the ones where the reinforcements are natural fibers, plays a vital role in mitigating this global issue. Green composite materials are already being embraced as an essential part of future manufacturing approaches [2, 3]. Sustainable composites are currently being used in applications where minor structural requirements are needed, like packaging industries and skin tissue engineering [4, 5]. In order to broaden their employment in semi-structural applications, as in the fields of automobile, transportation, and medical equipment, the parts produced must have acceptable mechanical properties and should be of a better dimensional and geometrical quality [6]. Appropriate material selection and primary processing techniques mainly influence the mechanical properties, whereas proper secondary processing/machining can determine the product's final dimensional and geometric stability [7, 8]. Among the available biodegradable polymers, extensive studies concerning the usage of poly(lactic acid) (PLA) as the matrix material for

sustainable composites are being carried out. These compostable thermoplastic polymers (as they emanate from potato, corn, and beet sugar) possess good mechanical properties comparable to synthetic polymers [9, 10] and hence are being investigated in this study as the matrix material.

Determining the optimal fiber reinforcement from biopolymers, like PLA, in order to fabricate eco-friendly and economically admissible functional composites is a critical task. Mahajan *et al.* [11] have employed a hybrid consolidated structure comprising various multi-criteria decision-making techniques to select the most acceptable fiber from the available natural fiber pool. The authors inferred that basalt fiber is the preferred choice by all techniques to deliver sustainable-green composites with mechanical properties appropriate for semi-structural utilization. Basalt fiber, classified as an eco-friendly natural fiber, has a 16% higher modulus, stronger alkaline resistance, similar tensile strength, increased interfacial adhesion, and is commercially available when compared to glass fiber. Also, basalt fibers are bio-inert, and their deformation at break is more than that of carbon fibers [12]. Although much literature has systematically documented the mechanical performance of different PLA-natural fiber composites, there is less attention on the systematic investigation of the development, and mechanical/microstructural characterization of basalt fiber reinforced PLA (BFPLA) composites.

Liu *et al.* [12] used a twin-screw extruder to prepare BFPLA composites with various concentrations of basalt fibers. The outcomes indicated that basalt fiber had a strong reinforcing and toughening influence than glass fiber. The same extrusion-injection molding method was also followed by Tábi *et al.* [13] and Deák and Czigány [14]. It was demonstrated that a renewable and sustainable composite with superior mechanical properties, eligible for engineering applications could be fabricated using basalt fiber reinforcement through injection molding. They have suggested that BFPLA composites could be utilized to produce technical parts with extreme precision, intricate design, and 3D shape. It was explained that by drying the materials properly, composites with higher mechanical properties might be produced. Deák and Czigány [14] also suggested that 30 wt% short basalt fiber reinforced PLA composite exhibited an impressive tensile and flexural strength, that were respectively 119.7 and 180.0 MPa. Unlike

other authors, Chatiras *et al.* [15] used basalt woven fabric for hot pressing/compression molding (film stacking method). This processing technique led to better mechanical properties as it avoided high shearing and fiber breakage, which occurs during extrusion and injection molding. This method provided composites with better fiber orientation and good fiber-matrix adhesion, and their tensile, flexural, and impact strength values were comparable with glass fiber mat composites. All these available studies suggest superior mechanical properties of BFPLA composites, making them an excellent sustainable alternative to glass/carbon fibers reinforced composites for specific applications. BFPLA composites are hence proved to be a good competitor for medium load applications, including laptop panels, two-wheeler visors, wheel hub covers on automobiles, *etc*.

Because of its convenience and simplicity, compression moulding is a popular cost-saving process for the primary manufacturing of composites. The fibre degradation caused by the intense thermomechanical processing that occurs during injection and extrusion moulding is avoided through the film stacking method, which also results in better-aligned fibres. As the result of this technique is in the form of laminate, cutting specimens for testing and further examination is substantial work.

The investigations to uncover the best sample cutting method from a laminate plate are given less attention in the literature. Researchers have tried to find the effect of edge trimming of the plates on their mechanical properties, primarily based on glass and carbon fiber reinforced polymer composites using different machining processes. Ghidossi *et al.* [16] examined the effect of cutting variables on the extent of damage and mechanical performance of off-axis glass/epoxy unidirectional specimens machined by side milling. The results showed that the machining parameters used to prepare the specimens significantly impacted their mechanical performance. The graphite/epoxy laminates were machined using three different cutting processes by Arola and Ramula [17], and it was found that the machined surface quality varied depending on the cutting method employed. However, there was no discernible difference in the laminate's bulk strength when subjected to bending loads. The stiffness of the graphite/bismaleimide laminate decreased with the magnitude of its surface roughness under fatigue loading [18].

In a flax-reinforced polymer composite, the dependency of the cutting tool and the method employed on delamination behavior was established [19]. The effect of defects produced by different machining techniques on the mechanical behavior of carbon fibre reinforced polymer composites was investigated, and it was concluded that the type and mode of mechanical loading affect composite mechanical response and favor a specific machining process [20]. Experiments were carried out to determine the effect of cutting methods on the mechanical properties of glass epoxy composites, and a correlation was established [21]. All these studies suggest the dependency of surface damage/delamination and mechanical properties on machining processes and various cutting tools. It is also crucial to note that fewer studies concerning sample preparation were available, and specifically, no examinations were based on sustainable composites.

The current experimental investigation is influenced by the requirement for cutting the samples from BFPLA laminates. The need to make the best samples with excellent mechanical properties motivated the authors to identify the best cutting method available. The present study hence aims to find out the best cutting process for sample making from a BFPLA laminate and to experimentally evaluate the effect of four different cutting tools/mechanisms (scroll saw, CNC milling machine, two-dimensional water jet cutting, and abrasive water jet cutting machine) on the tensile and flexural properties of the specimen. A comparative study has also been performed with BFPLA composites prepared from unidirectional and bidirectional basalt fabric mats. Furthermore, the results have been validated and substantiated through stereomicroscope analysis and microstructure examination using a field emission scanning electron microscope (FE-SEM).

2. Experimental procedure
2.1. Materials
PLA, which is used as the matrix material (3052-D, Natur-tec, Minnesota, USA), possesses a density of 1.24 g·cm^{-3} and a melt temperature of 147 °C, is 100% compostable, and meets ASTM D6400 and EN 13432 standards. The bi-directional basalt fabric consists of woven unstitched yarns (600-114, GBF Basalt Fiber Co. Ltd., Zhejiang, China) and uni-directional basalt fabrics (600-112, GBF Basalt Fiber Co. Ltd., Zhejiang, China) are employed to fabricate two types of BFPLA laminates. The complete properties of the selected basalt fibers (taken from the technical data sheet) are given in Table 1.

2.2. Processing of BFPLA laminates
Before the processing of laminates, the basalt fabric is cut into rectangular shapes (25 cm × 24 cm) and dried in a hot air oven at 90 °C for 24 hours. PLA granules are dried for 6 hours at 60 °C to remove the majority of the absorbed humidity. The optimum parameters for processing individual PLA sheets and composites were identified through pilot experiments.

Individual thin PLA sheets with an average thickness of 1 mm are manufactured by hot compression molding at 150 °C. The pressure is applied periodically, starting with 0.5 MPa for 3 minutes of contact time, then increasing to 4 MPa at a steady temperature for the next two minutes. At 60 °C, the sheets are cooled under pressure and removed.

In order to manufacture laminates, basalt fabric mats and polymer sheets are stacked one on top of the other in a metallic mold. The complete assembly is hot-pressed at 180 °C for 8 minutes with an initial pressure of 4 MPa. The pressure is then increased to 6 MPa for 2 minutes, followed by cooling of laminate under pressure. Laminates with an average thickness of 4 mm are ejected from the mold at a temperature of 60 °C. This method avoids fiber breakage caused by shear stresses induced by the melt-mixing procedure while simultaneously optimizing fiber orientation. One BFPLA laminate is developed using 5 PLA sheets and 4 basalt fiber mats. The same method is used to process both bidirectional and unidirectional laminates. The fiber weight fraction of

Table 1. Properties of the basalt fabric used.

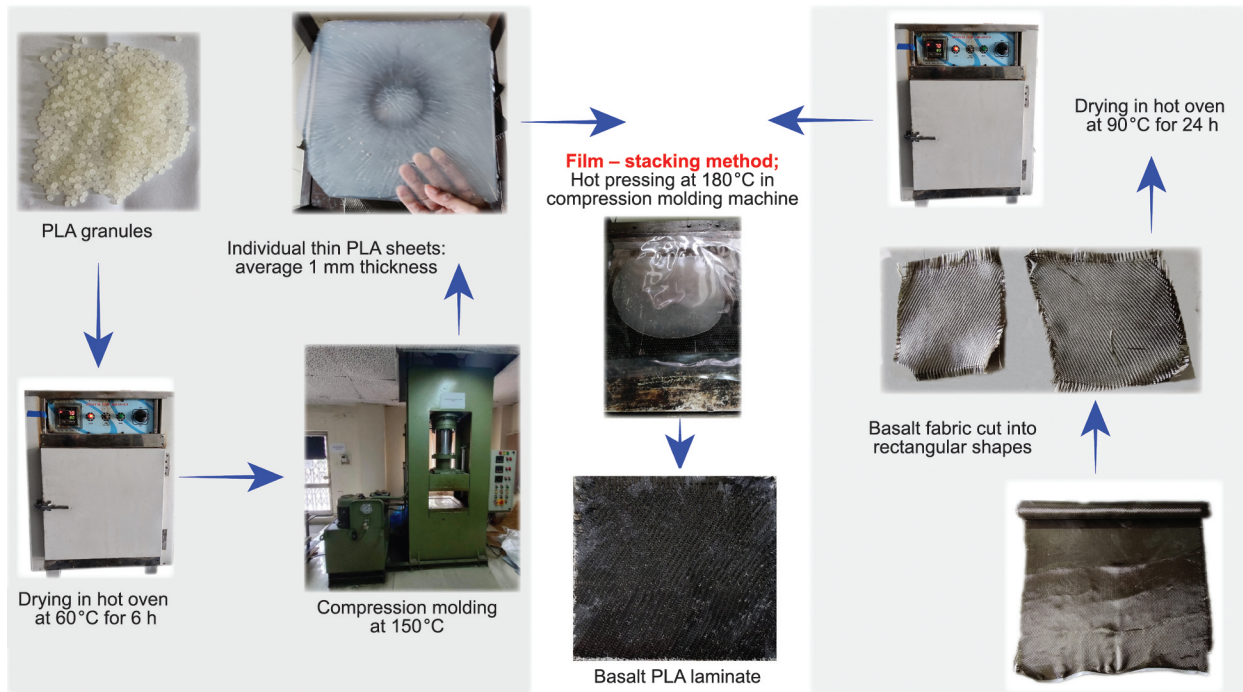|	Weft & Warp yarn specification [Tex]	Weft & Warp picks [ends/10 mm]	Woven pattern	Thickness [mm]	Tensile strength [MPa]	Areal density [g·m^{-2}]
Bidirectional basalt fabric	132	5×5	Twill	0.45	2100	480
Unidirectional basalt fabric	300	5	Unidirection	0.39	2100	400

Figure 1. Primary processing of BFPLA laminates.

unidirectional laminates is kept constant at 21% and that of bidirectional composites at 26%. The complete procedure is schematically shown in Figure 1.

2.3. Cutting processes

Four alternative procedures are used to cut samples from laminates (Figure 2). The specifications of the

Figure 2. Machines used for cutting samples. (a) MAKITA SJ401 variable speed scroll saw, (b) 5 inch scroll saw blade (c) Carvey CNC milling machine (d) Milling machine spindle (e) Solid carbide single flute upcut end mill (f) KMT waterjet system (g) Ultra-high pressure pump (h) Abrasive cutting head.

machine used and machining settings are explained in the following sections.

2.3.1. Scroll sawing
The variable speed scroll saw (SJ401, Makita, Aichi, Japan) with a throat depth of 406 mm and a stroke length of 18 mm is employed. All samples are cut using a 5 inch saw blade with 70 tooths per inch (TPI) and a stroke per minute (SPM) of 1200.

2.3.2. CNC milling
A CNC milling machine (Model: Carvey 3D, Inventables Inc., Chicago, USA) equipped with a solid carbide single flute upcut end mill (cutting diameter: 1/8 inch) is used for cutting BFPLA laminates. EASEL software is used to make the 3D design and input the feed rate and cutting depth. Feed rate, depth per pass, and plunge rate are set to the standard values of 1016 mm/min, 0.8 mm, and 304.8 mm/min, respectively.

2.3.3. The water jet and abrasive water jet cutting
The water jet and abrasive water jet cutting are done on a 45 kW Streamline Pro-III model (KMT waterjet systems, Auf der Laukert, Germany) having ultra-high pressure intensifier pumps of 6200 bar. All waterjet machining experiments were done with the abrasive waterjet nozzle to eliminate the impact of nozzle configuration on machining. Abrasive is added to the waterjet in the mixing chamber, and during waterjet operations, the abrasive entrance of the nozzle was blocked to prevent air from entering the jet and reduce cutting efficiency. The following standard cutting parameters were established for all specimens: feed rate of 1000 mm/min, stand-off distance of 3 mm, traverse rate of 250 mm/min, garnet abrasive materials, the abrasive flow rate of 200 gm/min during piercing, the abrasive flow rate of 150 gm/min while cutting, and a waterjet nozzle orifice diameter of 75 microns.

2.4. Mechanical testing
The mechanical properties (tensile and flexural) of the cut BFPLA specimens were evaluated and examined in terms of strength and modulus on a Universal Testing Machine (UTM) (Instron: 5982, USA) in accordance with ASTM D3039 and ASTM D7264 standards. A loading rate of 2 mm/min and a gauge length of 50 mm was set for tensile testing, while a span length of 60 mm was set for the flexural test, which was carried out using a 3 point bending fixture. To determine the failure process, the testing procedure was also recorded using a 1080p video camera at 60 fps (with 6 part lens quality and 64MP).

2.5. Stereomicroscope and microstructural analysis
The BFPLA specimens cut using various machining methods are observed under a stereomicroscope (Model: SMZ-745T, Nikon). Also, to depict the morphology of the surface and the topographical trends, microstructure analysis of the machined area is performed using a Field Emission-Scanning Electron Microscope (FE-SEM) (Model: Sigma 500, Zeiss Ultra Plus, Jena, Germany). Before micrographs were taken, a thin layer of gold was applied to the specimen using a sputter coater (BAL-TEC-SCD-005) to enhance its conductivity. This study can help determine and correlate the effect of surface defects with different cutting processes on the mechanical behavior of developed biocomposites.

The complete methodology followed for this study is shown in Figure 3. The nomenclature used to name and identify the different specimens machined using the various cutting processes is given in Table 2.

3. Results and discussion
3.1. Cutting of specimens and microstructural analysis
3.1.1. Scroll saw
A reciprocating pin end (hardened, high carbon steel) 5 inch blade with 70 TPI, with small round gullets and a lower feed rate, is used to reduce the burning effect and provide a comparatively better surface finish. The images of UDLS, UDTS, and BDS specimens and their magnified view captured using a stereomicroscope are shown in Figures 4a–4c, respectively. As the scroll saw threads the sharp reciprocating blade through the workpiece, the energy of the cut is converted into heat. Because the laminates are cut along the fiber direction in UDLS specimens, less force was required to cut the specimen than in other specimens. Cutting deformation and friction resulted from the blade's reciprocating movement, the material's limited thermal conductivity, and the lack of coolant resulted in increased heat generation during the cutting operation. This has led to a greater impact effect between the workpiece and the sawblade, as well as increased cutting resistance and cutting vibration.
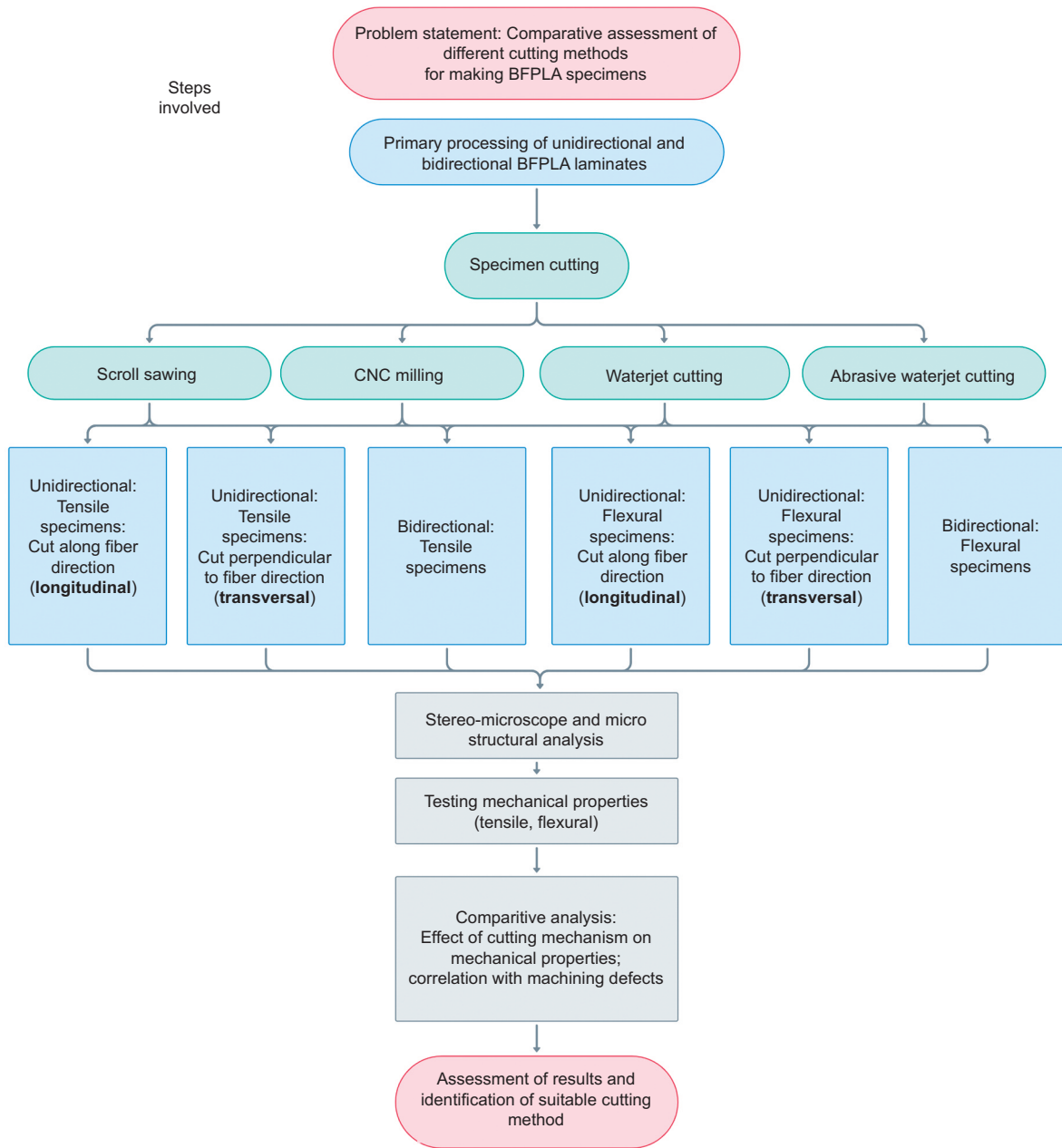
Figure 3. Research methodology employed.

Table 2. Nomenclature used for specimens machined using various cutting processes.

| Nomenclature	Details
UDLS	Unidirectional laminate specimen cut along the fiber direction (longitudinal) using scroll saw
UDTS	Unidirectional laminate specimen cut perpendicular to fiber direction (transversal) using scroll saw
BDS	Bidirectional laminate specimen cut using a scroll saw
UDLM	Unidirectional laminate specimen cut along the fiber direction (longitudinal) using a milling machine
UDTM	Unidirectional laminate specimen cut perpendicular to fiber direction (transversal) using a milling machine
BDM	Bidirectional laminate specimen cut using a milling machine
UDLW	Unidirectional laminate specimen cut along the fiber direction (longitudinal) using waterjet
UDTW	Unidirectional laminate specimen cut perpendicular to fiber direction (transversal) using waterjet
BDW	Bidirectional laminate specimen cut using waterjet
UDLAW	Unidirectional laminate specimen cut along the fiber direction (longitudinal) using abrasive waterjet,
UDTAW	Unidirectional laminate specimen cut perpendicular to fiber direction (transversal) using abrasive waterjet
BDAW	Bidirectional laminate specimen cut using abrasive waterjet
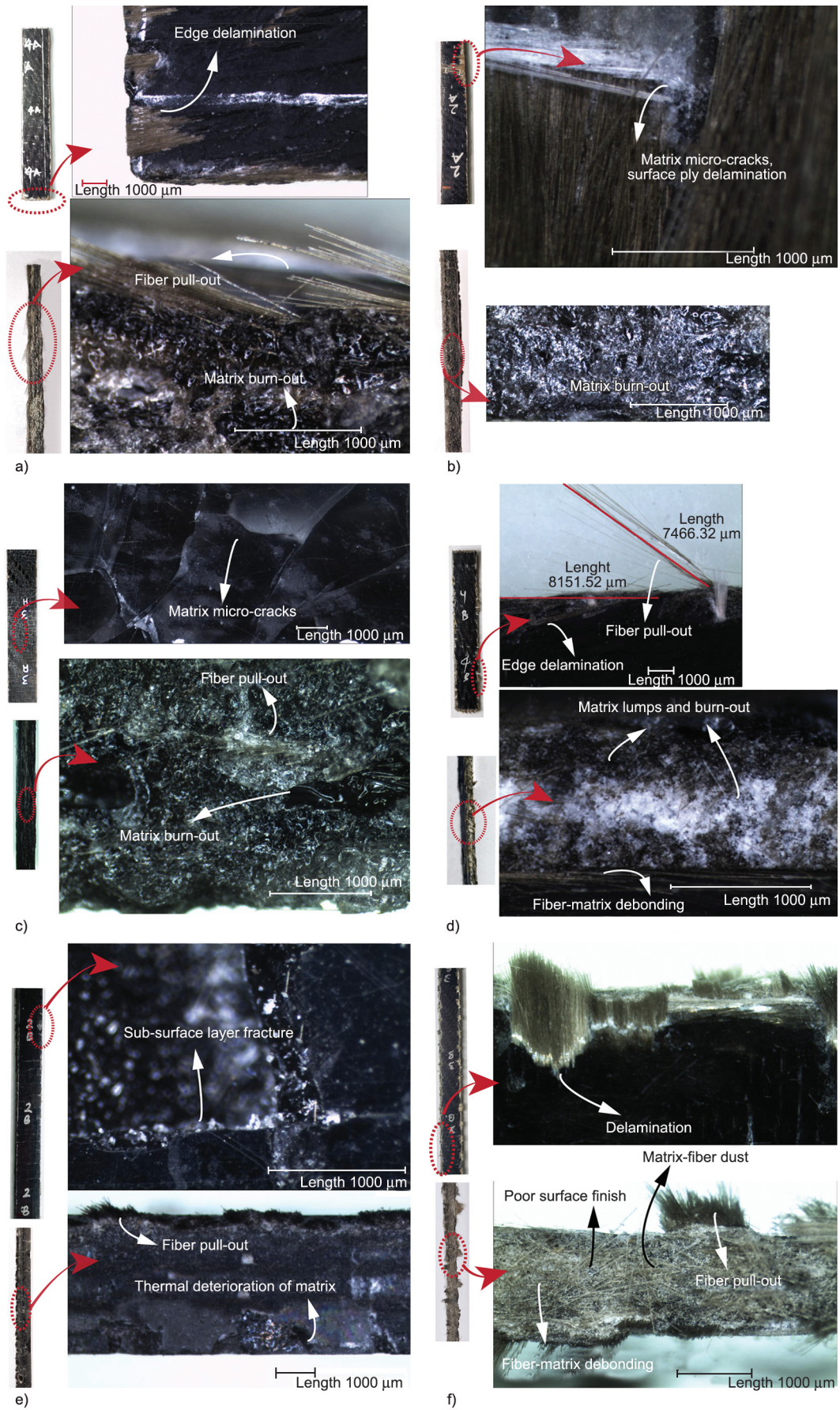
Figure 4. Specimens stereomicroscopy images cut by scroll saw and milling machine: (a) UDLS (b) UDTS (c) BDS (d) UDLM (e) UDTM (f) BDM.

Based on the magnified images of UDTS and BDS specimens, significant matrix burn-out and microcracks may be seen. Surface ply delamination is common for all three types of specimens. Fiber pull-out is significant in UDLS and has led to a visually poor surface finish.

Another critical observation during cutting using a scroll saw is that the PLA matrix melts and solidifies during the cutting process and leaves a glossy texture on the machined face. This can be observed clearly in the FE-SEM micrograph of BDS at 250× magnification. (Figure 6a). The melted PLA matrix sticks onto the sawblade pulling out fibers, resulting in voids, matrix fiber debonding, and reduced tool life. This is found prominent in cutting BDS samples and has resulted in cracked surfaces of the top matrix (PLA) layer.

3.1.2. CNC milling

A solid carbide single flute upcut end mill bit is employed, which assists in high-speed milling and high-volume removal of work material while creating a substantially better surface finish than two and three flute bits. The pictures of UDLM, UDTM, and BDM specimens and their magnified view obtained using a stereomicroscope are presented in Figures 4d–4f, respectively. When the bit first enters the laminate during the milling operation, friction at the start of the cut generates an excessively work-hardened layer in the workpiece. Fiber–matrix debonding, edge delamination, fiber disintegration, and pull-out of fibers are frequent forms of defects observed during the evaluation of all milled specimens. FE-SEM analysis of BDM (Figure 6b) also confirms the fibre damage in the form of breaking, bending, and cluster formation. The abrasive characteristics of the basalt fibers have produced substantial wear on tools contributing to subsurface damage in the specimens. For the BDM specimen, the micro-flaws, subsurface layer fractures, and increased surface roughness attributable to fiber/matrix dust linked with machining resulted in poor surface quality. The generation of elevated temperatures while machining has led to the softening and thermal deterioration of PLA. The burning of the matrix is more evident in UDTM specimens, whereas UDLM specimens reveal lumped matrix on the machined surface. Also, the UDLM specimens displayed a reduced rough surface as compared to the UDTM and BDM specimens.

3.1.3. Waterjet cutting

The images of UDLW, UDTW, and BDW specimens and their magnified view captured using stereomicroscope are shown in Figures 5a–5c, respectively. The developed heat from the machining micro-zone is swiftly dispersed since the water may function as a coolant in addition to its machining operation. This leads to the decreased build-up of heat, and consequently, thermal degradation of the matrix is negligible in all the waterjet cut specimens. This also leads to decreased delamination and inhibition of fiber debonding to some degree. UDLW exhibits minute cracks in the matrix top layer at a few spots, though not as much as in the longitudinal specimens cut using a scroll saw and CNC milling.

The machined surfaces are usually striated, consisting of crevices marking the erosion track of the water jet, which is very much evident on UDLW and UDTW specimens. UDTW displays a unique machined surface with micro matrix lumps found around the cut fibers. This may be attributed to the heat created when performing a transverse cut of fibers resulting in the quick melting and cooling of the PLA matrix. Small matrix lumps are also observed on BDW specimens but do not follow a patterned structure as seen on UDTW specimens. The FE-SEM micrographs of the BDW specimen (Figure 6c) reveal a substantially improved surface quality, with laminate layers clearly visible and distinguishable. Micrographs also demonstrate the minimal fiber pull-out and suppression of fiber disintegration, however, the waviness pattern caused by the jet deflection route is noticeable. Fiber roll-out damage is observed in the UDLW specimens. The term 'roll-out' refers to the final separation of fibers from their matrix area [22]. This may be generated by high-pressure jet stresses acting on the bare fibers within the machined zone. The fibres that have been broken or partially de-bonded from the matrix may be dislodged by incident jet pressures [23]. Bare fibers are also visible in BDW specimens, which resulted from the erosion of the enclosing matrix material. Micrographs show the fracture of fibers caused by the elevated water jet pressure on fibers. Hence the predominant material removal process visible in water jet cutting of BFPLA laminate, which is also confirmed by FE-SEM characterization, is the material failure associated with fibre breakage and matrix erosion.
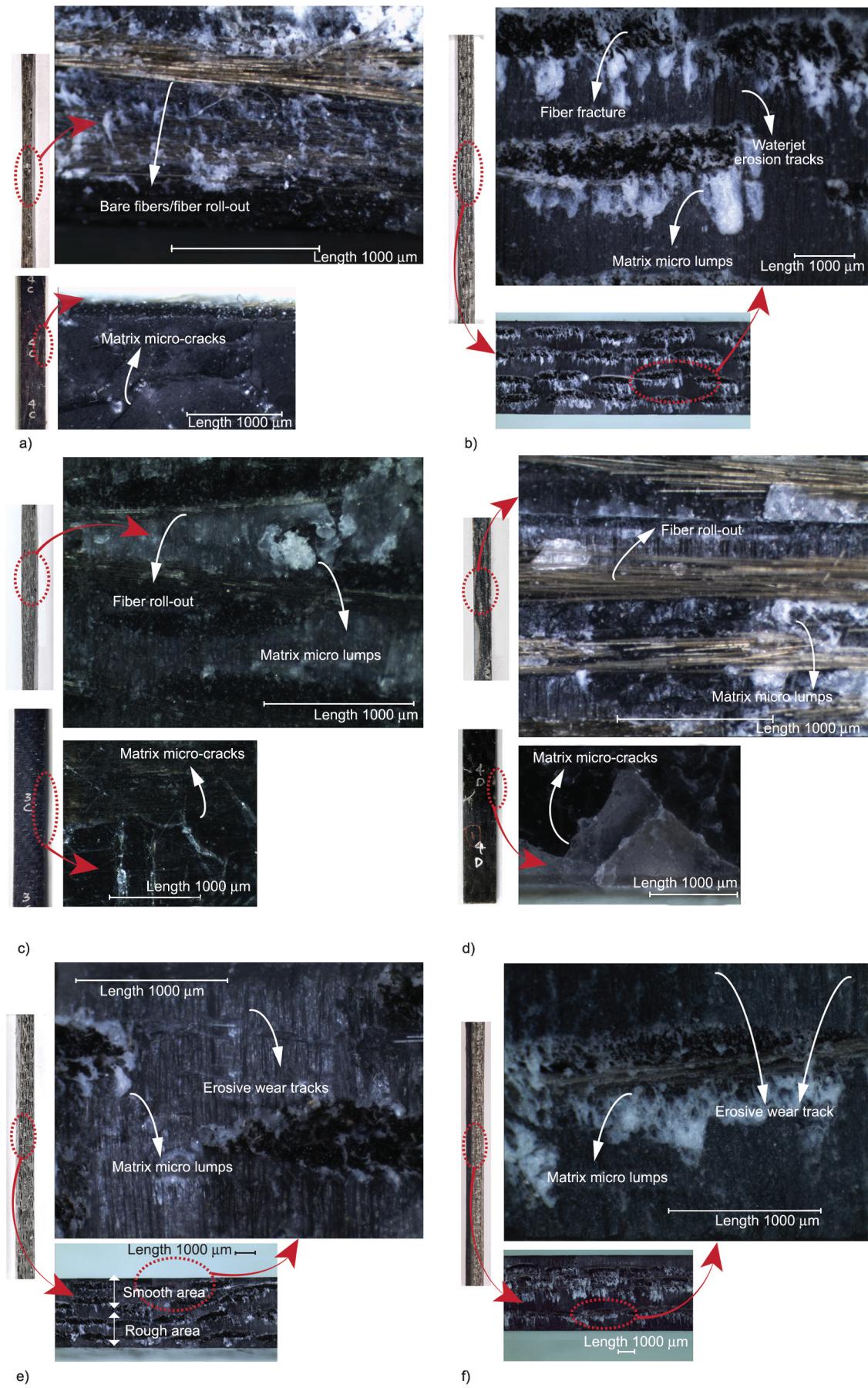
Figure 5. Specimens stereomicrocopy images cut from BFPLA laminate: (a) UDLW (b) UDTW (c) BDW (d) UDLAW (e) UDTAW (f) BDAW.

3.1.4. Abrasive waterjet cutting

The principal material removal technique in abrasive waterjet cutting is erosion by solid abrasive particles. Micro-cutting (cutting deformation or ploughing deformation), brittle fracture, melting, and fatigue are four subprocesses outlined by Meng *et al.* [24] that act concurrently and whose supremacy is governed by process parameters.

The images of UDLAW, UDTAW, and BDAW specimens and their microscopic view are shown in Figures 5d–5f, respectively. For all the specimens, the cutting front observations reveal the erosive wear tracks in the top zone of the cutting region and the formation of material lips towards the end of the tracks. Errant abrasive particles catapulting through the periphery of the coherent jet create these wear grooves. Also, the upper section displays a zone of smooth surface, and the bottom part indicates a comparably rougher area.

3.1.5. Microstructural analysis of the BDS, BDM, BDW, and BDAW specimens

Nonetheless, for all the specimens, regardless of fiber type and cutting direction, abrasive waterjet machining delivered consistently better and uniform surface profiles than all of the other machining methods employed, and the machined area is reasonably smooth, with no texture unevenness across the specimen depth. Although shallow abrasive wear tracks can be spotted on the FE-SEM micrographs of the BDAW specimen (Figure 6d), the waviness patterns as found on the BDW specimen were missing here. Minor levels of fibre pull-outs are also identified, although the degree of damage found is much lower than that observed with the other three processes. Like in waterjet cutting, matrix burning and thermal damage are negligible in abrasive waterjet specimens as well. One notable feature discovered in abrasive water jet specimens is that a damage zone/matrix
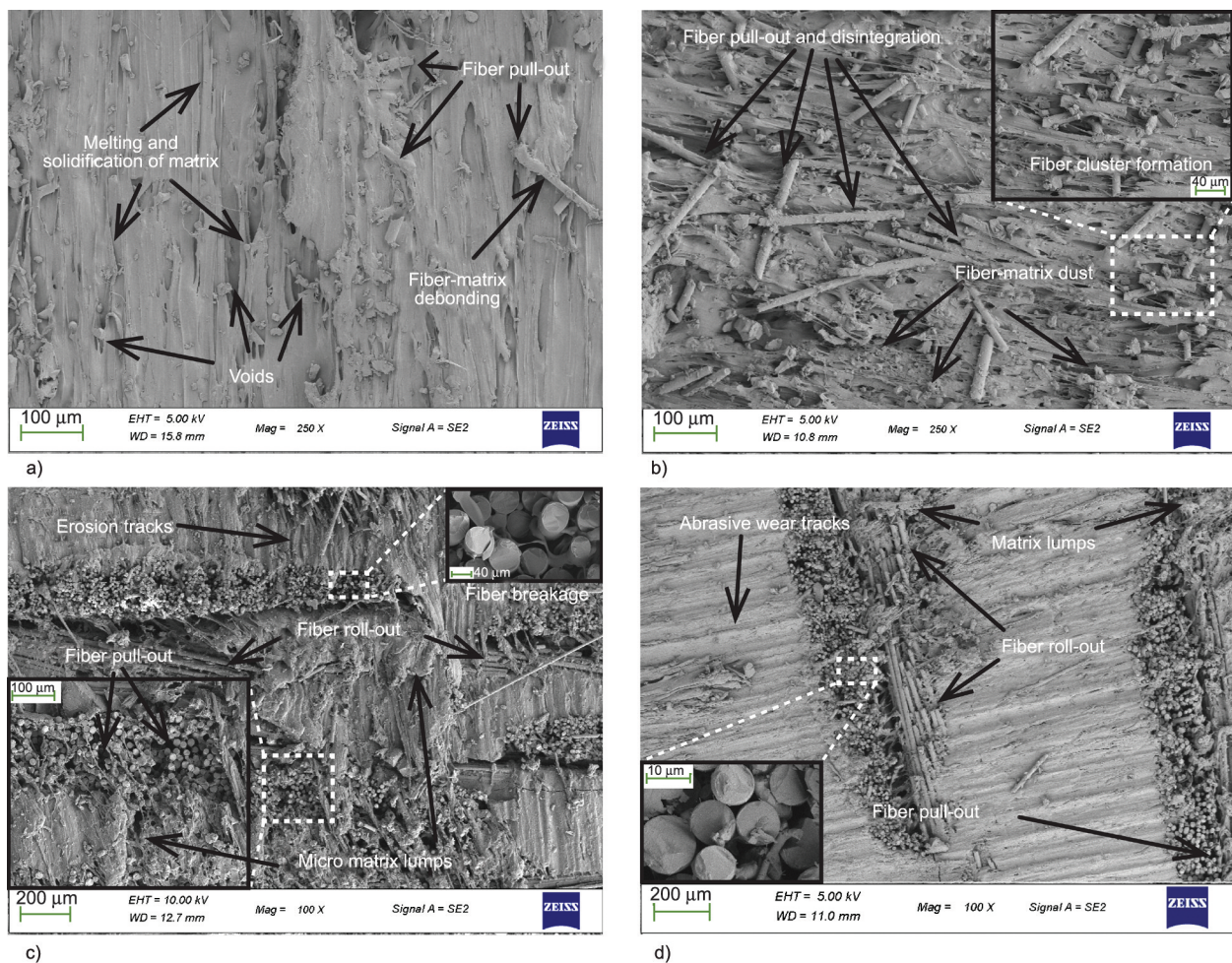

Figure 6. FE-SEM micrographs of the machined region of specimens: (a) BDS (b) BDM (c) BDW (d) BDAW.

fracture is present at the top layer margins and is much more evident on the UDLAW samples, which may be due to the impact of high-energy abrasives on laminate. Evidently, these were not so dominant in water jet specimens. In UDLAW specimens, little fiber roll-out is observed, although the frequency and degree of roll-out are much lower than what is observed in waterjet machined specimens. The decreased magnitude of the force acting on the machining zone is reflected in the lower amount of fiber roll-out. FE-SEM analysis suggests that the micromachining effects of abrasives and consequent matrix erosion are the dominating material removal process. These material removal mechanisms also assist towards a more consistent surface with reduced roughness and variability than the waterjet machined area. Interestingly like the UDTW samples, tiny matrix lumps are seen surrounding the cut fibers in BDAW specimens. Whereas the UDTAW samples demonstrate no/fewer lumps formation, much of the matrix around the fibers on the machined area is still intact. In comparison to other cutting processes,

abrasive waterjet samples did not show significant material degradation to either the fiber or matrix.

3.2. Tensile and flexural testing

All specimens are tested to obtain strength and modulus under tensile and flexural loading conditions at room temperature. The results obtained are plotted and shown in the Figure 7. The specimens show a specific trend in strength values. Clearly, the abrasive waterjet specimen showed the highest tensile strength value for all unidirectional (longitudinal), unidirectional (transversal), and bidirectional variants and the specimens obtained using CNC, while milling showed the least. Water jet specimens displayed the second-highest value, followed by the scroll saw specimens. The same trend is followed for flexural strength as well.

The abrasive water jet cut specimens showed a percentage increase of 27.9, 70.2, and 54.4% for the tensile strength values of unidirectional longitudinal, transversal and bidirectional, respectively, compared to the tensile strength values of specimens cut through
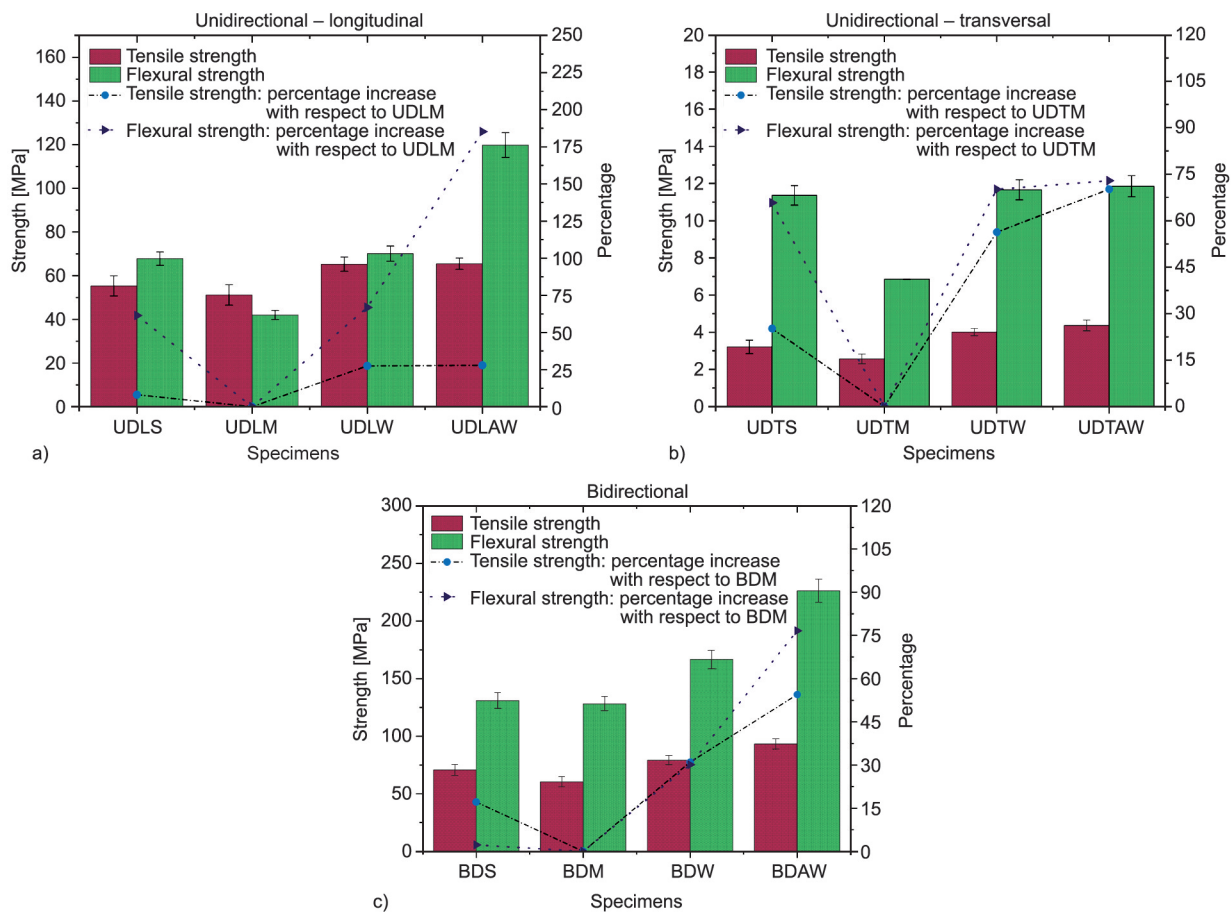

Figure 7. Tensile and flexural strength values of (a) unidirectional – longitudinal specimens (b) unidirectional – transversal specimens (c) bidirectional specimens.

CNC milling. Furthermore, when flexural strength values of unidirectional longitudinal, transversal and bidirectional specimens were compared to those of CNC milled specimens, the abrasive water jet cut specimens exhibited a percentage increase of 185.2, 72.9, and 76.6, respectively. The bidirectional specimen exhibited the maximum improvement of 17.9% when the tensile strength of specimens cut using abrasive waterjet was compared to the waterjet cut specimen, while the unidirectional longitudinal specimen showed the least improvement with only a 0.3% gain. In contrast, the abrasive waterjet cut unidirectional longitudinal specimen displayed a 70.9% rise in results when compared to the waterjet cut specimen for flexural strength.

The FESEM analysis and microscopy studies of milled specimens revealed the generation of elevated temperatures and matrix burning on milling cut specimens. This might have resulted in the fiber-matrix debonding in specimens, resulting in a reduction in strength and deterioration of the structural integrity. This may impair the tensile strength of specimens as well. Also, it was evident from the micrographs that the scroll saw cut specimens showed extensive fiber pull-out and matrix-fiber debonding. This machining-induced damage might have resulted in reduced mechanical properties. The matrix burning and thermal damage were negligible in abrasive waterjet and waterjet cut specimens. Also, on abrasive waterjet specimens, the degree of fiber pull-out was much lower than what was seen in waterjet machined specimens, which might have resulted in their better mechanical strength.

According to the mechanical characteristics of PLA-based composites reported in the literature, the flexural strength of the flax fiber (50 wt%) reinforced PLA laminate was 215 MPa, while the tensile strength of the banana (40 wt%)/ PLA biocomposites was 78.6 MPa [25]. The PLA/glass laminates offered tensile and flexural strengths of 108.2 and 99.4 MPa, respectively [15]. Flexural strength of 180.0 MPa was obtained for the PLA composite with 30% short basalt fiber reinforcement [14]. In this study, the bidirectional sample specimens cut with an abrasive waterjet yielded the highest tensile and flexural strength values of 93.28 and 226.2 MPa, respectively, which are better than those found in the literature. It is now evident that the abrasive water jet cut samples exhibit the key characteristics of a material removal method for use in composites, particularly BFPLA laminates.

The tensile and flexural modulus values followed a similar trend as the strength values as shown in Figure 8. Abrasive water jet cut specimens showed better elasticity than the rest of the specimens. Also, it was found that the unidirectional longitudinal cut specimens showed better stiffness (tensile modulus of 3017.5 MPa and flexural modulus of 17237 MPa) than bidirectional laminates. Prior work has documented the dependence of modulus values with regard to machining. According to Abidi et al. [26], the delamination defects and cut specimen surface quality caused Young's modulus values of carbon fiber reinforced polymer laminate to vary with respect to the machining processes. Sjögren et al. [27] demonstrated that defects, particularly fiber breakages,
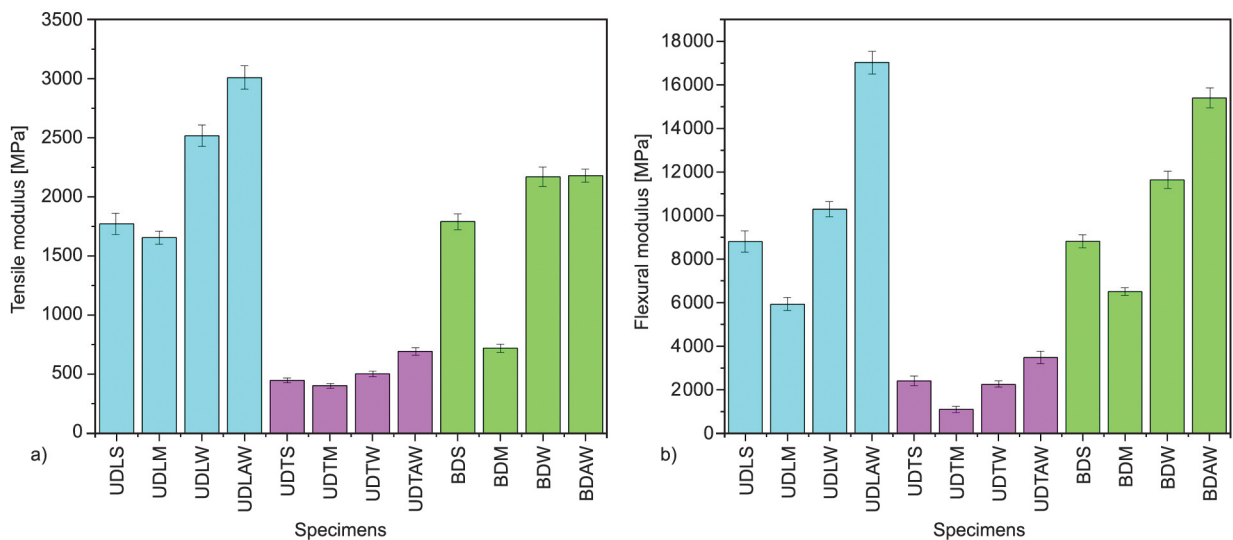

Figure 8. (a) Tensile modulus of tested specimens (b) flexural modulus of tested specimens.

influence the elastic modulus of an impact-damaged composite laminate. Cutting end-surface roughness and microcracks have been connected to changes in a material's loading stiffness and modulus values [28, 29]. A greater elastic modulus indicates a stiffer and typically more brittle material, which is less malleable and this suggests that bidirectional samples have comparatively better ductile properties along with higher ultimate strength values than other variants, particularly abrasive waterjet machined samples.

3.3. Failure analysis

The stress-strain curves of specimens machined using an abrasive waterjet are shown in Figure 9. The failure process at the macroscopic laminate level is explained via images from the captured film. Fracture is the full breakdown of the laminate's continuity, and it always begins with the commencement of a crack, followed by crack propagation. Figures 10a–10h demonstrate the tensile testing stages of the bidirectional specimen. As the load reached about 41 MPa, the top and bottom matrix layers formed additional microcracks, along with the initial cracks developed during machining. At the stress value of 45 MPa, the number of cracks began to increase, and minor fiber breakages (which are aligned in the transverse direction) emerged. As loading progressed, the concentration of these microcracks grew, and as the stress reached about 70 MPa, the matrix fractures coalesced, followed by fiber-matrix debonding, resulting in more fiber pull-outs. When the matrix breaks, the basalt fibers carry the stress, resulting in little dip and rise on the illustrated curve.

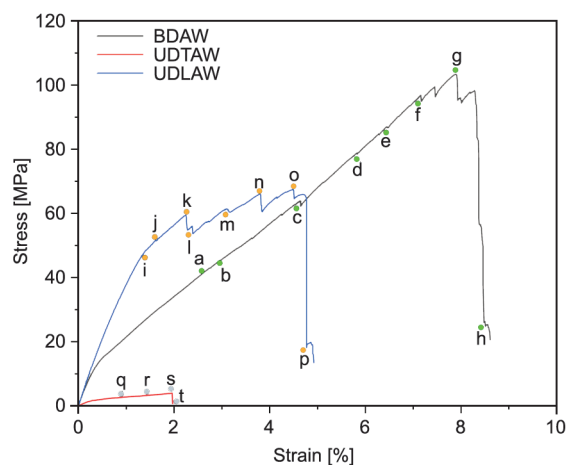As one can see, the failure of one layer affects the stiffness and residual strength of the laminate but

does not always result in total failure. This type of failure may occur due to a low interlaminar shear strength; cracks in one layer will turn along these interfaces, isolating the initially cracked layer from the other laminae, and the laminate will proceed to carry the load with slightly reduced stiffness and residual strength. Furthermore, Dharan [30] proposed that the original matrix crack might leave the fiber intact via crack bridging for brittle fibers in a brittle matrix. When both the matrix and the fiber are brittle, the fibers stay intact while the matrix fracture propagates around them, as in a glass-epoxy composite. At 84 MPa, the matrix completely fails. Interply failures (delamination) tend to predominate at about 94 MPa, combined with fiber breakage, resulting in total laminate failure at 103 MPa. The final failed specimen is depicted in Figures 10u and 10v.

Figures 10i–10p depict the failure process in a unidirectional longitudinal specimen machined using an abrasive water jet. At about 45 MPa, the initial failure appears in the form of a fiber break, which is accompanied by a failure of the surrounding matrix by transverse cracking that extends up to the neighboring fibers and fiber debonding. The size of these failure spots stays essentially the same as the load increases, but their number increases throughout the specimen, causing additional weakening. As the load rises to 58 MPa, the number of isolated fractures increases, providing a weaker route for fracture on the specimen's sides. With increasing stress, fiber failures accelerate, eventually resulting in the coalescence of fiber breaks through transverse cracking followed by interfacial shearing at 66 MPa. Figures 10w and 10x exhibit the UDLAW specimen that failed.

The failure process of unidirectional transversal specimen cut using abrasive waterjet is shown in Figures 10q–10t. UDTAW specimens exhibited typical brittle fracture behavior, with nearly constant stress (3.67 MPa) during cracking, rapid crack propagation, and negligible deformation. This might be because, when the specimen was pulled in the direction normal to the fiber, the Poisson effect in the matrix causes significant shear stress at the fiber ends, causing the bond to break. The matrix has fractured in a cleavage mode, as seen in Figures 10y, $10z_1$, and $10z_2$, while the fibers have remained almost intact. Another interesting data to be noted is that the tensile and flexural strength, as well as the elastic modulus values of transverse cut specimens, show a considerable reduction compared to the longitudinal ones.
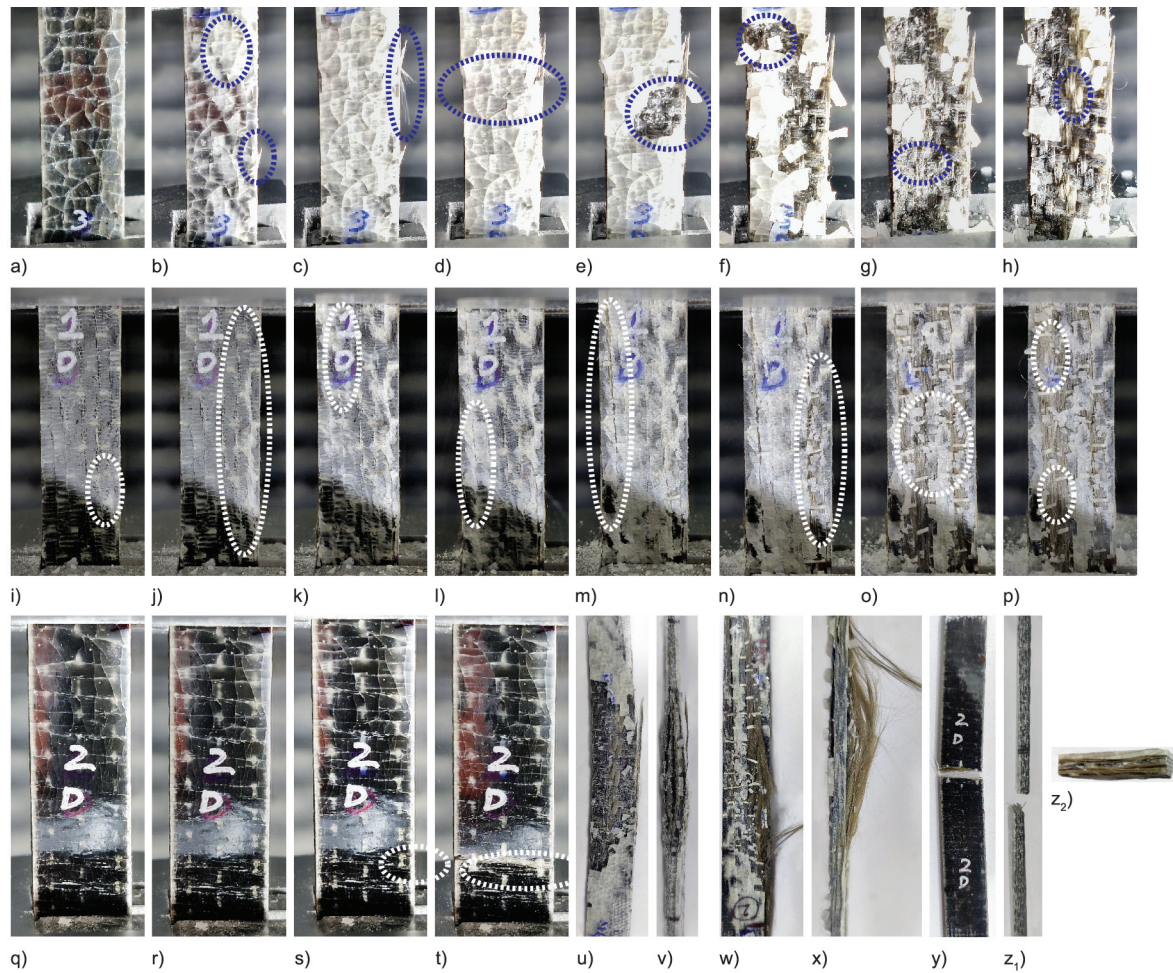

Figure 9. Stress-strain curves of abrasive waterjet machined specimens.

Figure 10. The tensile testing stages of abrasive waterjet machined specimens, (a to h) failure process of BDAW, (i to p) failure process of UDLAW, (q to t) failure process of UDTAW, (u, v) top view and side view of failed BDAW, (w, x) top view and side view of failed UDLAW, (y–z_2) top view and side view of failed UDTAW.

Patel and Dave [31] reported a decrease in tensile strength of specimens with higher fiber orientation angle/cutting direction (45°) and a better tensile strength for specimens (longitudinal) with 0° fiber orientation angle.Ramulu and Arola [22] have observed a 97% reduction in strength values, and Cordin *et al.* [32] have reported an 88% decrease for specimens cut at 90° to the fiber orientation. In our experiments, the transversal specimens showed an average of 94% reduction in tensile strength and 85% reduction in flexural strength values compared to the longitudinal ones. This shows that changes in the fiber orientation angle can lead to a considerable weakening of the material. Despite significant improvements in mechanical characteristics along the fiber direction, the strength values in the transverse direction are inferior to those of pure PLA material. This also supports the anisotropic behavior of the processed BFPLA. The elastic modulus of unidirectional laminates can be theoretically calculated by

the rule of mixtures. A modified micromechanical model [33, 34] for the prediction of elastic modulus is given below (Equation (1)):

$$E_c = \kappa \eta_d \eta_l \eta_0 V_f E_f + V_m E_m \tag{1}$$

where κ is the fiber area correction factor, η_d is the fibre diameter distribution factor, η_l is the fibre length distribution factor, η_0 is the fibre orientation distribution factor, E_x is the elastic modulus, V_x is the volume fraction with the subscript c, f and m being composite, matrix, and fiber, respectively. According to Equation (1), the parameter η_0 quantifies the impact of fiber alignment with respect to the load applied. It is calculated using the equation given below (Equation (2)):

$$\eta_0 = \sum_n a_n \cos^4 \theta_n \tag{2}$$

This clearly illustrates that if the cutting direction is 90°, cosθ will be zero, implying that basalt fibres will make no contribution to the stiffness of the laminate. Furthermore, the reinforcing fibres in the 90° orientation reduce the rigidity of the laminate, which may be justified by the ease with which basalt and PLA debond, leading to significantly lower strength and modulus values.

4. Conclusions

The current experimental investigation aims to determine the optimal cutting process for cutting specimens from a BFPLA laminate. Additionally, a comparative assessment is reported for composites with unidirectional and bidirectional basalt fabric mats. The following are the primary conclusions of the present research endeavor.

- The abrasive nature of basalt fibers resulted in significant tool wear, resulting in subsurface damage and increased surface roughness, according to the stereomicroscope and FE-SEM analysis of milled specimens. The high-temperature values and matrix burning resulted in matrix-fiber debonding in milled specimens, reducing strength and structural integrity.

- Microscopy and microstructural analysis revealed considerable fiber pull-out and matrix-fiber debonding in the scroll saw cut specimens. Thermal deterioration of the matrix is minimized in all waterjet cut specimens, resulting in decreased delamination and mitigation of fiber debonding to a certain extent. Material failure owing to fiber fracture and matrix erosion is the principal mechanism of material loss in water jet cutting of BFPLA laminates.

- Abrasive waterjet machining consistently generated significantly uniform surface profiles as compared to other methods across all specimens, independent of the fiber type or cutting direction. The machined area was generally smooth, with no texture unevenness over the specimen depth. Matrix burning, thermal degradation, and fiber roll-out were reduced due to the minimal force exerted in the machining zone. The primary material removal mechanisms seem to be abrasive micromachining and matrix erosion.

- In all unidirectional (longitudinal), unidirectional (transversal), and bidirectional variants, the abrasive waterjet specimen provided the highest tensile strength, while the CNC machined specimen had the lowest. Water jet specimens had the second-highest value, followed by scroll saw specimens. A similar trend exists for flexural strength values.

- The abrasive waterjet cutting effectively generated bidirectional BFPLA specimens with the highest tensile and flexural strengths of 93.28 and 226.2 MPa.

It is concluded that the choice of cutting technique has a substantial influence on the strength of cut samples, and abrasive water jet cutting is the best approach for producing better quality BFPLA samples with smooth, uniform surface profiles, fewer defects, and improved mechanical properties. Future research may focus on quantifying machining damages on a sustainable composite and expanding the evaluation of the impacts of machining damages on fatigue and impact strength. A correction criteria index may also be generated for predicting the actual strength of laminates produced when samples are cut using traditional cutting methods.

Acknowledgements

References

[1] Silva A. L. P., Prata J. C., Walker T. R., Campos D., Duarte A. C., Soares A., Barcelò D., Rocha-Santos T.: Rethinking and optimising plastic waste management under COVID-19 pandemic: Policy solutions based on redesign and reduction of single-use plastics and personal protective equipment. Science of the Total Environment, **742**, 140565 (2020).
https://doi.org/10.1016/j.scitotenv.2020.140565

[2] Mohanty A. K., Vivekanandhan S., Pin J-M., Misra M.: Composites from renewable and sustainable resources: Challenges and innovations. Science, **362**, 536–542 (2018).
https://doi.org/10.1126/science.aat9072

[3] Mohd-Ishak Z. A., Ahmad-Thirmizir M. Z.: Producing green composites via polymer blending. Express Polymer Letters, **15**, 910–911 (2021).
https://doi.org/10.3144/expresspolymlett.2021.73

[4] Verma N., Pramanik K., Sing A. K., Biswas A.: Design of magnesium oxide nanoparticle incorporated carboxy methyl cellulose/poly vinyl alcohol composite film with novel composition for skin tissue engineering. Materials Technology, **37**, 706–716 (2021).
https://doi.org/10.1080/10667857.2021.1873634

[5] Arrieta M. P., Beltran F., Abarca de las Muelas S. S., Gaspar G., Sanchez Hernandez R., de la Orden M. U., Urreaga J. M.: Development of tri-layer antioxidant packaging systems based on recycled PLA/sodium caseinate/recycled PLA reinforced with lignocellulosic nanoparticles extracted from yerba mate waste. Express Polymer Letters, **16**, 881–900 (2022).
https://doi.org/10.3144/expresspolymlett.2022.64

[6] Jani S. P., Kumar A. S., Khan M. A., Kumar M. U.: Machinablity of hybrid natural fiber composite with and without filler as reinforcement. Materials and Manufacturing Processes, **31**, 1393–1399 (2016).
https://doi.org/10.1080/10426914.2015.1117633

[7] Jaeschke P., Kern M., Stute U., Haferkamp H., Peters C., Herrmann A. S.: Investigation on interlaminar shear strength properties of disc laser machined consolidated CF-PPS laminates. Express Polymer Letters, **5**, 238–245 (2011).
https://doi.org/10.3144/expresspolymlett.2011.23

[8] Komanduri R.: Machining of fiber-reinforced composites. Machining Science and Technology, **1**, 113–152 (2007).
https://doi.org/10.1080/10940349708945641

[9] Akintayo O. S., Olajide J. L., Betiku O. T., Egoh A. J., Adegbesan O. O., Daramola O. O., Sadiku E. R., Desai D. A.: Poly(lactic acid)-silkworm silk fibre/fibroin biocomposites: A review of their processing, properties, and nascent applications. Express Polymer Letters, **14**, 924–951 (2020).
https://doi.org/10.3144/expresspolymlett.2020.76

[10] Wang F. Y., Dai L., Ge T. T., Yue C. B., Song Y. M.: α-methylstyrene-assisted maleic anhydride grafted poly (lactic acid) as an effective compatibilizer affecting properties of microcrystalline cellulose/poly(lactic acid) composites. Express Polymer Letters, **14**, 530–541 (2020).
https://doi.org/10.3144/expresspolymlett.2020.43

[11] Mahajan A., Binaz V., Singh I., Arora N.: Selection of natural fiber for sustainable composites using hybrid multi criteria decision making techniques. Composites Part C: Open Access, **7**, 100224 (2022).
https://doi.org/10.1016/j.jcomc.2021.100224

[12] Liu T., Yu F., Yu X., Zhao X., Lu A., Wang J.: Basalt fiber reinforced and elastomer toughened polylactide composites: Mechanical properties, rheology, crystallization, and morphology. Journal of Applied Polymer Science, **125**, 1292–1301 (2012).
https://doi.org/10.1002/app.34995

[13] Tábi T., Tamás P., Kovács J. G.: Chopped basalt fibres: A new perspective in reinforcing poly(lactic acid) to produce injection moulded engineering composites from renewable and natural resources. Express Polymer Letters, **7**, 107–119 (2013).
https://doi.org/10.3144/expresspolymlett.2013.11

[14] Deák T., Czigány T.: Chemical composition and mechanical properties of basalt and glass fibers: A comparison. Textile Research Journal, **79**, 645–651 (2009).
https://doi.org/10.1177/0040517508095597

[15] Chatiras N., Georgiopoulos P., Christopoulos A., Kontou E.: Thermomechanical characterization of basalt fiber reinforced biodegradable polymers. Polymer Composites, **40**, 4340–4350 (2019).
https://doi.org/10.1002/pc.25295

[16] Ghidossi P., El-Mansori M., Pierron F.: Influence of specimen preparation by machining on the failure of polymer matrix off-axis tensile coupons. Composites Science and Technology, **66**, 1857–1872 (2006).
https://doi.org/10.1016/j.compscitech.2005.10.009

[17] Arola D., Ramula M.: Machining-induced surface texture effects on the flexural properties of a graphite/epoxy laminate. Composites, **25**, 822–834 (1994).
https://doi.org/10.1016/0010-4361(94)90143-0

[18] Arola D., Williams C. L.: Surface texture, fatigue, and the reduction in stiffness of fiber reinforced plastics. Journal of Engineering Materials and Technology, **124**, 160–166 (2002).
https://doi.org/10.1115/1.1416479

[19] Slamani M., Karabibene N., Chatelain J-F., Beauchamp Y.: Edge trimming of flax fibers and glass fibers reinforced polymers composite – An experimental comparative evaluation. International Journal of Material Forming, **14**, 1497–1510 (2021).
https://doi.org/10.1007/s12289-021-01644-6

[20] Haddad M., Zitoune R., Eyma F., Castanié B.: Influence of machining process and machining induced surface roughness on mechanical properties of continuous fiber composites. Experimental Mechanics, **55**, 519–528 (2015).
https://doi.org/10.1007/s11340-014-9967-y

[21] Matur M. S., Kori S. A., Rao R. M. V. G. K.: Comparative analysis of cutting effect on mechanical properties and microstructural behavior of glass epoxy composites. AIP Conference Proceedings, **2057**, 020061 (2019).
https://doi.org/10.1063/1.5085632

[22] Ramulu M., Arola D.: Water jet and abrasive water jet cutting of unidirectional graphite/epoxy composite. Composites, **24**, 299–308 (1993).
https://doi.org/10.1016/0010-4361(93)90040-f

[23] Sheikh-Ahmad J. Y.: Nontraditional machining of FRPs. in 'Machining of polymer composites' (ed.: Sheikh-Ahmad J. Y.) Springer, Boston, 237–291 (2009).
https://doi.org/10.1007/978-0-387-68619-6_6

[24] Meng H. C., Ludema K. C.: Wear models and predictive equations: Their form and content. Wear, **181**, 443–457 (1995).
https://doi.org/10.1016/0043-1648(95)90158-2

[25] Ranakoti L., Gangil B., Mishra S. K., Singh T., Sharma S., Ilyas R. A., El-Khatib S.: Critical review on polylactic acid: Properties, structure, processing, biocomposites, and nanocomposites. Materials, **15**, 4312 (2022).
https://doi.org/10.3390/ma15124312

[26] Abidi A., Salem S. B., Bezazi A., Boumediri H.: A comparative study on the effect of milling and abrasive water jet cutting technologies on the tensile behavior of composite carbon/epoxy laminates. Mechanics of Composite Materials, **57**, 539–550 (2021).
https://doi.org/10.1007/s11029-021-09978-7

[27] Sjögren A., Krasnikovs A., Varna J.: Experimental determination of elastic properties of impact damage in carbon fibre/epoxy laminates. Composites Part A: Applied Science and Manufacturing, **32**, 1237–1242 (2001).
https://doi.org/10.1016/s1359-835x(01)00058-6

[28] Meng K. P., Chai C. G., Sun Y. L., Wang W., Wang Q. Y., Li Q. M.: Cutting-induced end surface effect on compressive behaviour of aluminium foams. European Journal of Mechanics - A/Solids, **75**, 410–418 (2019).
https://doi.org/10.1016/j.euromechsol.2019.02.015

[29] Cooper R. C., Bruno G., Onel Y., Lange A., Watkins T. R., Shyam A.: Young's modulus and Poisson's ratio changes due to machining in porous microcracked cordierite. Journal of Materials Science, **51**, 9749–9760 (2016).
https://doi.org/10.1007/s10853-016-0209-9

[30] Dharan C. K. H.: Fracture mechanics of composite materials. Journal of Engineering Materials and Technology, **100**, 233–247 (1978).
https://doi.org/10.1115/1.3443485

[31] Patel H. V., Dave H. K.: Effect of fiber orientation on tensile strength of thin composites. Materials Today: Proceedings, **46**, 8634–8638 (2021).
https://doi.org/10.1016/j.matpr.2021.03.598

[32] Cordin M., Bechtold T., Pham T.: Effect of fibre orientation on the mechanical properties of polypropylene–lyocell composites. Cellulose, **25**, 7197–7210 (2018).
https://doi.org/10.1007/s10570-018-2079-6

[33] Virk A. S., Hall W., Summerscales J.: Modulus and strength prediction for natural fibre composites. Materials Science and Technology, **28**, 864–871 (2013).
https://doi.org/10.1179/1743284712y.0000000022

[34] Cullen R. K., Singh M. M., Summerscales J.: Characterisation of natural fibre reinforcements and composites. Journal of Composites, **2013**, 416501 (2013).
https://doi.org/10.1155/2013/416501